Biotribology 20 (2019) 100110

Contents lists available at ScienceDirect

Biotribology

journal homepage: www.elsevier.com/locate/biotri

Low force, high noise: Isolating indentation forces through autocorrelation analysis

Christopher S. O'Bryan[a], Kyle D. Schulze[b], Thomas E. Angelini[a,c,d,*]

[a] Department of Mechanical and Aerospace Engineering, Herbert Wertheim College of Engineering, University of Florida, Gainesville, FL, United States
[b] Department of Mechanical Engineering, Samuel Ginn College of Engineering, Auburn University, Auburn, AL, United States
[c] J. Crayton Pruitt Family Department of Biomedical Engineering, Herbert Wertheim College of Engineering, University of Florida, Gainesville, FL, United States
[d] Institute of Cell & Tissue Science and Engineering, Herbert Wertheim College of Engineering, University of Florida, Gainesville, FL, United States

ARTICLE INFO

Keywords:
Contact mechanics
Micro-indentation
Nano-indentation
Hydrogel characterization

ABSTRACT

Simple contact models are often used in combination with indentation measurements to determine the elastic moduli of materials in the limits of small strain and linear-elastic deformation. However, for soft biological samples these limits can occur at indentation forces comparable to detection noise from the instrument. Here we describe a data analysis method for determining the moduli of soft materials when the measured forces are comparable to the level of instrumental noise; relationships between the force and displacement autocorrelation functions enable the elastic modulus to be determined from indentation curves with large uncertainties in the measured force. In simulations of force-displacement indentation data using the Hertz and Winkler foundation contact models with added noise, we find the autocorrelation analysis enables the accurate measurement of known elastic moduli, even when the noise-to-signal ratio is large throughout an indentation experiment. We also find that this analysis method is more accurate at measuring the modulus at high noise levels compared to directly fitting the model curve to the data. We further validate this approach experimentally by testing a series of polyacrylamide hydrogel slabs prepared within a wide polymer concentration range, finding the measured modulus to be in agreement with the moduli determined through rheological characterization.

1. Introduction

Measuring the elastic moduli of soft materials is an essential part of numerous areas in science and engineering focused on soft and biological matter. For example, in cellular biomechanics research, characterizing the material properties of soft hydrogels, polymers, biopolymers, and entire cells is necessary to guide our understanding of cell behavior; cell motility, focal adhesion strength, and differentiation are influenced by the elasticity of the cell's microenvironment [1–3]. To this end, many experimental indentation techniques have been applied to measuring the moduli of soft materials, each with varying levels of sensitivity [4–11]. For example, micro-indentation techniques measure forces on the order of μN with noise levels on the order of 100 nN at indentation depths of 10–100 μm [6,10]. By comparison, nano-indentation techniques, such as colloidal probe AFM, will measure forces on the range of nN with noise levels on the order of piconewtons at indentation depths of 1–10 nm [5,8]. The effectiveness of these techniques to accurately measure moduli of soft materials depends on the quality of the data and the application of the appropriate contact model to account for indenter geometry, sample thickness, and material behavior [10].

The first models to capture the relationships between indentation force and material deformation were developed by Bousinessq and Hertz for two linear-elastic half-spaces loaded under small strains [12–15]. Tabor, and later Oliver and Pharr, applied these contact models to experimentally measure the elastic modulus of hard metals by analyzing the unloading portion of the indentation curve [16–18]. This approach separates elastic response from plastic deformation by leveraging the material behavior of hard metals which yield at low strains (~0.2%) and exhibit linear-elastic responses during unloading [8,16,19]. However, soft materials are capable of undergoing large strain deformation without yielding and often exhibit non-linear behavior at relatively moderate strains that is not captured by the linear elastic contact models of Bousinessq and Hertz [20–24]. Thus, the Oliver and Pharr method of analyzing the unloading portion of indentation curves to determine a material's linear elastic modulus is not

* Corresponding author at: Department of Mechanical and Aerospace Engineering, Herbert Wertheim College of Engineering, University of Florida, Gainesville, FL, United States.
E-mail address: t.e.angelini@ufl.edu (T.E. Angelini).

https://doi.org/10.1016/j.biotri.2019.100110
Received 5 June 2019; Received in revised form 14 October 2019; Accepted 21 October 2019
Available online 30 October 2019
2352-5738/ © 2019 Elsevier Ltd. All rights reserved.

applicable to indentation measurements of soft materials that exhibit large deformation without yielding.

The inability to use the Oliver and Pharr approach to determine elastic moduli of typical soft materials suggests that indentation measurements should be analyzed in the linear elastic regime. This approach has been demonstrated for measuring the material properties of soft materials, including polymeric networks [10,25,26], silicone elastomers [27,28], and biomaterials [6,29,30]. However, for even softer materials, the small strain limit in which traditional contact models remain valid, up to 10% for example, the noise level in the measured forces may exceed the elastic forces. Consider the indentation of an $E^* = 1$ kPa material with $\pm$ 1 μN of random noise in the measured force. For the elastic response force to exceed this noise level given an $R = 1000$ μm radius of curvature indentation tip, the material must first undergo approximately 9% strain. Similarly, for colloidal-probe AFM measurements with an $R = 5$ μm indentation tip, the same material must reach about 14% strain before the indentation force exceeds a 100 pN noise level in the measured force. In both cases, indentation measurements in the linear regime are dominated by noise and prohibit determining a soft material's elastic modulus. To accurately measure the material properties of such soft materials from indentation measurements in the linear-elastic regime, new data analysis techniques to isolate indentation forces from the noise in the measurement are necessary.

Here, we present a data analysis approach for measuring the elastic moduli of soft materials within the linear deformation regime using autocorrelation functions of the displacements and applied forces measured from an indenting instrument during a typical normal loading experiment. This method isolates the indentation force from the instrumental noise, allowing modulus measurements to be performed when the indentation force is comparable to the uncertainty in the measured force. To explore the limits of this analysis approach, we simulate indentation curves with increasing levels of Gaussian noise and compute the force and displacement autocorrelation functions. With this analysis method we can accurately measure the elastic moduli from noisy data, even when the noise-to-signal ratio is large throughout an indentation experiment. In addition, we investigate the effects of a force offset and uncertainty in the point of contact on the measured modulus. We further validate this approach through micro-indentation experiments on polyacrylamide (pAAm) hydrogel samples and find measured moduli that agree with rheological characterization within a factor of two.

2. Materials and methods

2.1. Simulated indentation curves

Simulated force-displacement indentation curves are produced using custom written MATLAB scripts. Here, we model a hemispherical indentation tip ($R = 1000$ μm) pressing against a flat, elastic substrate having a composite modulus of $E^* = 25$ kPa. To simulate the displacement of the indentation tip, we create an array of points from zero to a final indentation depth with step size of 0.01 μm. This step size corresponds to a displacement rate of 1 μm/s with sampling frequency of 100 Hz. At each displacement location, we determine the indentation force by applying either the Hertz or Winkler foundation contact model for a sphere on flat contact. A normal distribution of random numbers with zero mean and standard deviation σ_n is superimposed on the indentation force to simulate experimental noise in the measurement.

2.2. Hydrogel sample preparation

To prepare hydrogel samples, solutions of acrylamide monomer (AAm) containing *N*,*N*′-methylenebisacrylamide (BIS) as a crosslinking agent, ammonium persulfate (APS) as an initiator, and tetramethylethylenediamine (TEMED) as an accelerant are prepared in ultrapure water (18.2 MΩ). Samples are prepared at the concentrations described in Table 1.

Table 1
Constituents of pAAm hydrogel samples and the fully swollen polymer concentrations for each sample after swelling to equilibrium in ultrapure water for 24 h. Values presented as weight percent of the solution or gel.

Sample no.	AAm	BIS	APS	TEMED	Fully swollen concentration
1	3.75	0.15	0.15	0.15	2.85
2	5.00	0.20	0.15	0.15	4.23
3	7.50	0.30	0.15	0.15	6.72
4	10.00	0.40	0.15	0.15	8.86

Hydrogel samples swell to equilibrium over 24 h before experimental characterization. Final polymer concentrations are determined by comparing the measured mass of hydrogels immediately after polymerization and after swelling for 24 h in ultrapure water.

2.3. Micro indentation measurements

Micro-indentation measurements are performed using a Bruker BioSoft indenter equipped with a 1 mm radius of curvature hemispherical glass borosilicate indentation tip. Indentation samples with a thickness of $h = 100$ μm are prepared on glass cover slips and allowed to swell in ultrapure water for 24 h to reach equilibrium conditions. Prior to indentations, the indentation tip is plasma cleaned and coated with 0.1 wt% F-127 Pluronic to mitigate the effects of adhesion. Samples are submerged in water and indentations are performed by vertically displacing the indentation tip at a rate of 1 μm/s to a final depth of $d = 10$ μm into the sample. The measured force and displacement of the indentation tip are captured at data acquisition rates of 100 Hz.

2.4. Rheological characterization

Rheological characterization of hydrogel samples are performed using an Anton Paar MCR 702 rheometer equipped with a 25 mm roughened plate-on-plate configuration with a 1 mm working gap. 1 mm thick pAAM samples are cast between glass microscope slides and allowed to swell for 24 h in ultrapure water to reach equilibrium conditions. Samples are subsequently loaded between the rheometer plates and trimmed to size. Small amplitude frequency sweeps are performed at 1% strain across a frequency range of 10^1–10^{-2} Hz.

2.5. Data analysis

All data analysis was performed using custom written MATLAB scripts. Autocorrelation functions were computed by employing MATLAB's FFT functions to compute the Fourier transforms of the data.

3. Results and discussion

3.1. Autocorrelation analysis approach

To analyze the indentation curves within the linear regime and in which a sample's elastic restoring force is comparable to the noise in the measured force, we consider an infinitely stiff hemispherical indentation tip brought into contact with a soft, flat substrate (Fig. 1a). In the case when the contact width is less than the thickness of the sample ($2a < h$), the Hertz contact model describes the relationship between the indentation force and the tip displacement, given by

$$F_H(t) = \frac{4}{3}E^* R^{1/2} d^{3/2}(t) = K_H d^{3/2}(t),$$

where $E^* = E/(1-\nu^2)$ is the composite modulus, E and ν are the Young's modulus and Poisson's ratio of the substrate, R is the radius of

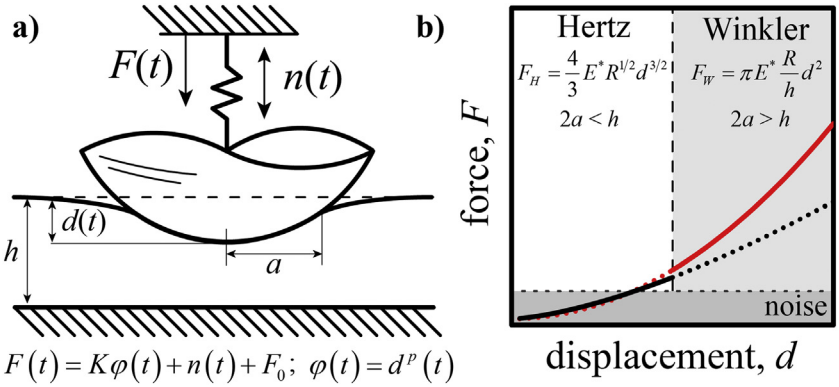

Fig. 1. Experimental motivation: a) The measured force of a hemispherical indenter tip in contact with an elastic substrate can be modeled by the general power law expression $F(t) = K\varphi(t) + n(t) + F_0$, where $\varphi(t)$ captures the displacement of the indentation tip, K is a constant dependent on the contact model being applied, and F_0 is the offset in the measured force. b) For thin samples, the Hertz contact regime is limited to the initial portion of the indentation curve in which the contact width is less than the sample thickness ($2a < h$); however, the indentation forces may be comparable to the noise in the measurement for soft, thin samples. Application of Winkler contact model in the higher force regime when the contact width exceeds the sample thickness ($2a > h$) requires prior knowledge of sample thickness to accurately measure E^*.

curvature of indentation tip, and d is the displacement of the indentation tip [13]. Although the linear elastic contact models are independent of time, the displacement of the indentation tip and corresponding indentation force are recorded as functions of time in experimental measurements. Here, we express F_H and d explicitly as functions of time to emphasize this temporal relationship, which we leverage below in our analysis.

For cases where the contact width is greater than the thickness of the sample ($2a > h$), the Winkler elastic foundation contact model predicts a different relationship between the indentation force and the tip displacement, given by

$$F_W(t) = \pi E^* \frac{R}{h} d^2(t) = K_W d^2(t),$$

where h is the thickness of the substrate [31]. For soft, thin, biological samples, the transition from the Hertz regime to the Winkler regime can occur when the indentation force is comparable to the noise in the measured force (Fig. 1b). To develop a formalism that includes the effects of noise and that can be used for either contact model, we introduce a generalized variable, $\varphi(t)$, where $\varphi(t) = d^{3/2}(t)$ in the Hertz regime and $\varphi(t) = d^2(t)$ in the Winkler regime. Substituting $\varphi(t)$ into either contact model provides a general expression for the indentation force, given by

$$F(t) = K\varphi(t) + n(t) + F_0,$$

where K is either K_H or K_W, $n(t)$ is the noise in the measured force, and F_0 accounts for offset errors in zeroing an instrument before measuring.

While autocorrelation functions are often used to identify periodic patterns in stationary random data, they may also be used to compare trends in non-stationary data. Here, we compare the trends of the measured force and displacement functions to isolate the indentation force from the noise in the measurement. The autocorrelation function of the time dependent force, $F(t)$, is given by

$$C_{FF}(\tau) = \langle F(t)F(t+\tau)\rangle_t,$$

where angle brackets indicate an average over experimental time, t, and τ is the shifting time variable. Similarly, the autocorrelation function of the entire right-hand side of our generalized force-displacement relationship is given by

$$\langle [K\varphi(t) + n(t) + F_0][K\varphi(t+\tau) + n(t+\tau) + F_0]\rangle_t.$$

Expanding the product and performing the averages yields a combination of nine auto- and cross-correlation functions given by

$$K^2 C_{\varphi\varphi}(\tau) + KC_{\varphi n}(\tau) + KC_{n\varphi}(\tau) + C_{nn}$$
$$(\tau) + KC_{F_0\varphi} + KC_{\varphi F_0} + C_{nF_0} + C_{F_0 n} + C_{F_0F_0},$$

where $C_{\varphi\varphi}(\tau)$ is the autocorrelation function of $\varphi(t)$, $C_{\varphi n}(\tau)$ and $C_{n\varphi}(\tau)$ are the cross correlation functions of $\varphi(t)$ and $n(t)$, $C_{nn}(\tau)$ is the autocorrelation function of $n(t)$. The noise in the system is random, thus the noise autocorrelation function should instantly de-correlate at lag times $|\tau| > 0$. Similarly, treating the noise function as a zero-mean random variable, the n-φ and φ-n cross-correlation functions are expected to be negligible, as will all other terms involving random noise. The remaining cross-correlation functions involving F_0 integrate to constant values because F_0 itself is a constant that factors out of the correlation integrals. We therefore group all these constants and represent them by a single variable, β, which we treat as a free fitting variable in our analysis below. Incorporating all these simplifications results in a linear relationship between $C_{FF}(\tau)$ and $C_{\varphi\varphi}(\tau)$, given by

$$C_{FF}(\tau) = K^2 C_{\varphi\varphi}(\tau) + \beta.$$

The composite modulus E^* can be measured by fitting a line to the C_{FF} vs $C_{\varphi\varphi}$ curve; the slope of the linear fit corresponds to the square of the constant K, in which E^* is implicit.

3.2. Simulated indentation curves

To investigate the capability of this analysis approach to determine elastic moduli from indentation measurements, we simulate force-displacement curves that correspond to a hemispherical indentation tip ($R = 1000\,\mu m$) pressing against an elastic substrate with a composite modulus of $E^* = 25\,kPa$. The indentation curve is simulated using the Hertz contact model to a depth of $d = 10\,\mu m$ corresponding to a maximum load of $F = 33.33\,\mu N$; noise in the measured force is simulated by adding normally distributed random numbers to the indentation force having zero mean and a standard deviation, σ_n (Fig. 2a). As σ_n increases, it becomes increasingly challenging to visually discern the elastic force-displacement trend from the noise (Fig. 2a). In these initial simulations, we set $F_0 = 0$; we explore the role of F_0 later. For each indentation curve, we calculate the autocorrelation functions of force and displacement, finding that C_{FF} and $C_{\varphi\varphi}$ appear to have the same shape as they decrease with increasing lag time (Fig. 2b,c). One notable difference between the curves is seen at $\tau = 0$, where we observe a dramatic spike in the force autocorrelation function, corresponding to the instantly de-correlating noise contribution. We measure the composite modulus E^* by plotting C_{FF} versus $C_{\varphi\varphi}$ and fitting a line through the linear portion of the curve while allowing for a vertical offset; the slope of the linear fit corresponds to the square of the constant K (Fig. 2d).

We repeat this process over a wide range of noise levels, simulating 100 indentation curves at each σ_n, finding the average value of E^* to be very close to the known value of 25 kPa (Fig. 3a). Even when the noise level is > 150% the maximum elastic force in the F-d curves, the average measured values of E^* are within 2% of the known value with a standard deviation within 20% of the known value. Furthermore, we find the average E^* values determined through the autocorrelation approach are closer to the known value of 25 kPa and have a smaller variance than those determined by directly fitting the Hertz contact model to the F-d indentation curve; direct model fitting of indentation curves with noise levels of 150% the maximum force result in a 25% error in E^* with over a 30% standard deviation (Fig. 3a). Furthermore,

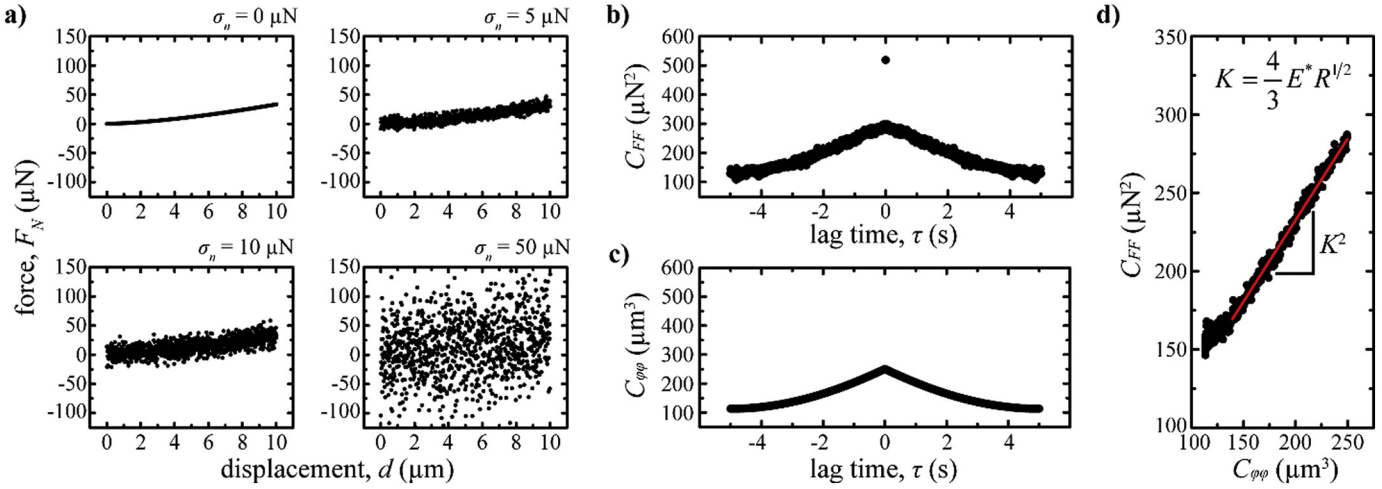

Fig. 2. Indentation simulations and autocorrelation analysis: a) Simulated indentation curves of samples having a composite modulus E^* = 25 kPa. Data are simulated using the Hertz contact model with added Gaussian noise at levels between σ_n = 0 μN and 50 μN. b) Force autocorrelation function (C_{FF}) of a simulated Hertz indentation with added random noise (σ_n = 15 μN). c) The corresponding displacement autocorrelation function ($C_{\varphi\varphi}$) in which $\varphi(t) = d^{3/2}(t)$ for the Hertz contact model. d) The composite modulus E^* is measured by plotting C_{FF} vs $C_{\varphi\varphi}$ and fitting a line to the linear portion of the curve.

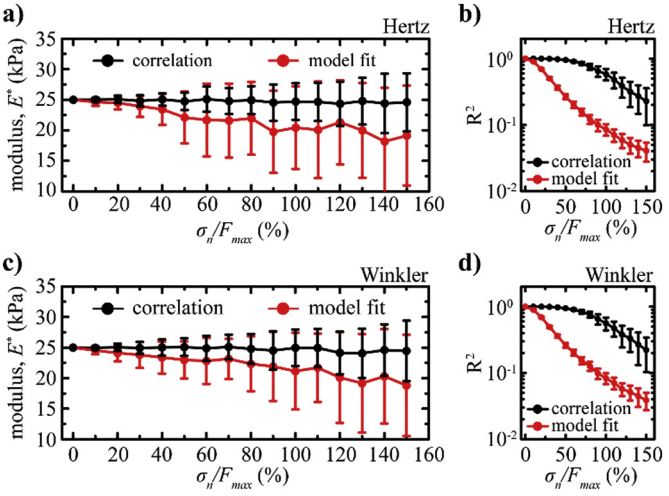

Fig. 3. Comparison between the autocorrelation analysis approach and a direct fit of the contact model: a) Measured E^* from *F-d* indentation curves simulated using the Hertz contact model with increasing levels of noise (σ_n) relative to the maximum indentation force (F_{max}). b) R^2 values demonstrate a higher confidence in the measured E^* values using the autocorrelation approach compared to directly fitting data with the Hertz model. c) Measured E^* values from *F-d* indentation curves simulated using the Winkler foundation contact model with increasing levels of noise. d) R^2 values demonstrate a higher confidence in the measured E^* values for the autocorrelation approach compared to directly fitting data with the Winkler foundation model.

we consistently find that this autocorrelation analysis produces elastic moduli with higher levels of confidence than when directly fitting model curves to noisy indentation data; R^2 values in fitting autocorrelation functions are found to be much larger than those produced when directly fitting data with a model curve (Fig. 3b). Indentation curves simulated using the Winkler foundation contact model under the same experimental conditions and with a sample thickness of h = 200 μm produce similar results; at noise levels > 150% the maximum indentation force, we can measure the moduli very close to the known value with standard deviations within 20% (Fig. 3c). Likewise, the E^* values determined using the autocorrelation approach were closer to the known value than those measured using a direct fit of the model and produced higher R^2 values (Fig. 3c,d). Thus, the autocorrelation method is suitable for analyzing data at extremely low levels of applied force where noise dominates the measurement.

3.3. Force and displacement error analysis

In general, uncertainty in the initial point of contact of the indentation tip and offsets in the measured force can lead to substantial errors when measuring E^* of soft materials [10]. Thus, we explore how these uncertainties in the force and displacement can produce errors in the measured modulus when applying our autocorrelation analysis method. The analysis described above indicates that the unknown force offset, F_0, does not interfere with determining E^*; F_0 only changes the offset, β. To test this hypothesis, we repeat the simulations described above where the noise level is set to σ_n = 5 μN, while imposing a 20 μN offset in the measured force (Fig. 4a). Force autocorrelation functions are determined for both the initial indentation curve (C_{FF}) and the indentation curve with an imposed offset ($C_{F'F'}$) (Fig. 4b). As expected, C_{FF} and $C_{F'F'}$ exhibit identical behavior and are separated by an offset in their magnitude; the full analysis using either F or F' finds the composite modulus to be E^* = 25.4 kPa. These results confirm that an offset in the measured force has no effect on measured modulus when using the autocorrelation analysis approach.

Unlike a force offset, an error in determining the initial point of contact of the indentation tip is expected to produce an error in the measured modulus. Uncertainties in determining the initial point of contact can arise from noise in the measured force. For example, one extreme method for estimating the initial point of contact is to determine the location when the measured force exceeds the noise level (Fig. 4c) [32]. However, this approach will overestimate the initial point of contact; for an R = 1000 μm indentation tip brought into contact with a E^* = 25 kPa substrate and ± 5 μN of noise in the measured force, one would overestimate the initial point of contact by approximately 3 μm. Previous investigations have found that this uncertainty in the point of contact enabled the fitting of the wrong contact model to data and produced errors in E^* up to 300% greater than the expected value [10].

To explore how uncertainties in the initial point of contact contribute to errors in the measured moduli using autocorrelation analysis, we simulate indentation curves using the Hertz contact model with an imposed offset in the displacement (d_0'), described by the relationship $F(t) = K_H(d(t) - d_0')^{3/2}$. Here we omit random noise from the simulated indentation data to isolate the contribution of a displacement offset on the measured moduli. For a given indentation depth, d_{max}, we determine the fractional error in the measured composite modulus,

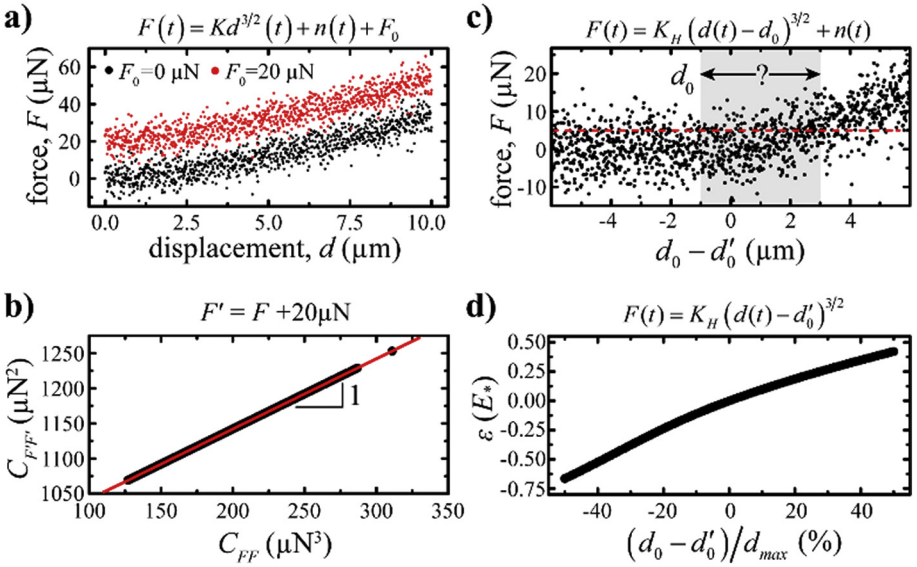

Fig. 4. Error analysis of force offset and initial point of contact: a) Simulated indentation curves using the Hertz model with a 20 μN offset in force to explore the effect of force offsets on the measured modulus. b) Autocorrelation functions of indentation curves have a 20 μN offset ($C_{F'F'}$) and 0 μN offset (C_{FF}) exhibit identical behavior indicating no change in the measure modulus resulting from a force offset. c) Noise in the indentation curve can result in uncertainty when determining the initial point of contact between the indentation tip and the substrate. d) Fractional error in the measured modulus $\varepsilon(E^*)$ using the autocorrelation analysis method is dependent on the uncertainty in the point of contact from the true point of contact ($d_0 - d_0'$) and the maximum depth of the indentation measurement (d_{max}).

$\varepsilon(E^*)$, for a given error in the initial contact location, $d_0 - d_0'$, where $d_0 = d(0)$ and d_0' is the true point of contact (Fig. 4d). When the detected contact point is assumed to occur prior to the true contact point ($d_0 < d_0'$), we find the measured modulus is underestimated. Likewise, the composite modulus is overestimated when the initial contact point is chosen after the true point of contact ($d_0 > d_0'$). Since E^* is found by analyzing data along the entire indentation curve, the magnitude of error in determining E^* is dependent on both the error in the initial point of contact and the depth of the indentation (d_{max}); the error in sured modulus can be reduced by decreasing the uncertainty in the initial point of contact or by increasing the indentation depth being analyzed. In the case analyzed here, < 10% error in E^* can be achieved if errors in d_0' relative to d_{max} are < 10%. For example, a 1 μm uncertainty in the initial point of contact for a maximum indentation depth of 3 μm results in a 28% error in the measured modulus; the same uncertainty for a d_{max} = 10 μm indent would only produce a 10% error in the measured modulus.

3.4. Experimental investigation

To test this autocorrelation analysis method on real indentation data, we perform indentation measurements on pAAm hydrogel slabs prepared at varying polymer concentrations, c, and with a thicknesses of $h \approx 100$ μm using a $R = 1000$ μm radius of curvature hemispherical glass indentation tip. If this hydrogel slab was much thicker we would estimate the linear regime of the indentation curve to be the first 10 μm. However, for such a thin slab, the transition from the Hertz contact regime to the Winkler contact regime is expected occur at $d \approx 2.5$ μm, where the full contact width becomes comparable to the 100 μm gel thickness. We therefore test the capabilities of our method by analyzing the first 2.5 μm of the indent on the thin slabs that should be described by the Hertz model, in principle. To estimate the initial point of contact of the indentation tip, we fit a line to a sub-set of data points beyond the point where the force first exceeds the noise in the measurement; the initial point of contact is taken to be the y-intercept of the fitted line. While the force-displacement indentation curves of relatively high polymer concentration samples within this regime have a low signal to noise ratio and may resemble a typical indentation curve (Fig. 5a), the indentation curves of lower polymer concentration samples have no discernable shape and resemble random noise (Fig. 5b). However, by computing the autocorrelation functions of the force and displacement function and plotting C_{FF} vs $C_{\varphi\varphi}$, we are able to isolate the indentation data from the noise and measure the E^* of the samples (Fig. 5c). Treating the hydrogel as incompressible with $\nu = 0.5$ [33], we determine the Young's modulus of each sample, finding $E = 2.12 \pm 0.22$ kPa, 7.80 ± 0.81 kPa, 28.55 ± 4.52 kPa, and 70.36 ± 5.28 kPa for the $c = 2.85$ wt%, 4.23 wt%, 6.72 wt%, and 8.86 wt% hydrogel samples, respectively.

We compare the results of our autocorrelation analysis approach to moduli values determined using oscillatory shear rheology on pAAM hydrogels prepared at the corresponding polymer concentrations. Small amplitude frequency sweeps are performed at 1% strain and the elastic shear modulus (G') is measured across a frequency range of 10^1–10^{-2} Hz (Fig. 5d). Consistent with the behavior of an elastic solid, we find G' to remain relatively flat across all frequencies tested. We relate the Young's modulus to the elastic shear modulus through the expression $E = 2G(1 + \nu)$, where we again assume the pAAm hydrogel samples are incompressible, having a Poisson's ratio of $\nu = 0.5$. From the rheological data, we determine the Young's modulus to be $E = 1.66 \pm 0.22$ kPa, 6.24 ± 0.16 kPa, 19.58 ± 4.37 kPa, and 47.16 ± 4.21 kPa for the $c = 2.85$ wt%, 4.23 wt%, 6.72 wt%, and 8.86 wt% pAAm hydrogel samples, respectively. We find these rheological results agree to within a factor of 2 with the indentation moduli values determined using the autocorrelation analysis approach for all concentration ranges explored (Fig. 5e). We note that the moduli values determined from indentation measurements appear to be consistently higher than those obtained from shear rheology. This discrepancy between the indentation and rheological measurements could arise from slight differences in sample preparation and fixturing, or uncertainties in the initial point of contact of the indentation measurements.

4. Conclusion

The Oliver and Pharr technique for analyzing indentation curves provides an elegant solution to decoupling elastic deformation from plastic flow and has become the standard for characterizing the material properties of hard materials [16,17]. In contrast to traditional engineering materials like metals, soft solids often do not yield or flow even at high strains and instead smoothly transition back and forth between linear and nonlinear elastic regimes of response [14,15,17]. Therefore, following the Oliver-Pharr method of analyzing the unloading portion of a force-indentation curve at large indentation depths, treating it as the residual linear elastic response, is not appropriate for characterizing many soft materials like crosslinked hydrogels. Thus, as we continue to characterize the material properties of soft, biological materials through indentation, new techniques and data analysis

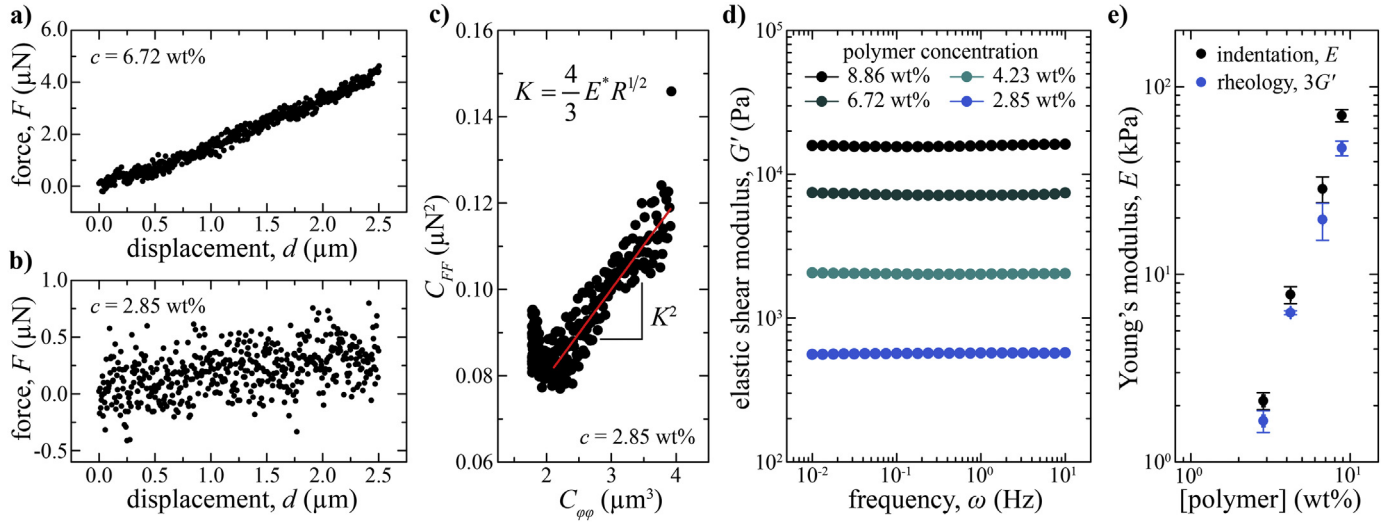

Fig. 5. Characterization of pAAm samples: a) Representative indentation curves of $c = 6.72$ wt% pAAm samples in the Hertz regime; measured force is approximately an order of magnitude higher than the noise. b) Representative indentation curve of $c = 2.85$ wt% pAAm sample in the Hertz regime; measured force is comparable to the noise. c) The composite modulus is determined by fitting a line to the linear portion of the C_{FF} vs $C_{\varphi\varphi}$ plot. d) The elastic shear modulus (G') of pAAm samples are measured using small amplitude frequency sweeps across a wide range of frequencies. e) Moduli values from autocorrelation analysis of indentation data is in good agreement with shear rheology measurements; measured moduli are within a factor of 2 for all polymer concentrations tested.

approaches will be necessary to overcome the unique challenges associated with materials having moduli several orders of magnitude lower than traditional engineering materials. The application of contact models that don't accurately capture the complex behavior of the material, the difficulties in accurately determining the surface location, and the challenge of analyzing data with large noise to signal ratios can lead to large uncertainties in accurately determining the material properties [10]. Here, we have presented a data analysis technique for decoupling the indentation force from the noise in the measured force using autocorrelation functions of the measured force and displacement. We find that this analysis approach is capable of accurately measuring moduli from indentation curves even in the extreme conditions where the uncertainty in the force exceeds the elastic response force. The ability to accurately measure material properties at high noise to signal ratios is beneficial for indentations measurements of soft biopolymer networks, living tissues, thin polymer coatings, soft polymeric gels, and other low moduli materials. Although we have focused our investigation on the contact of a hemispherical indentation tip, this analysis approach remains valid for any indentation tip geometry in which the indentation force and displacement can be related through a power law, including flat punches and conical indentation tips.

Acknowledgement

The authors thank Anton Paar for the use of the Anton Paar 702 rheometer through their VIP academic research program. Funding for this work was provided by Alcon Laboratories.

Declaration of competing interest

The authors have no conflicts of interest to declare.

References

[1] D.E. Discher, P. Janmey, Y. Wang, Tissue cells feel and respond to the stiffness of their substrate, Science. 310 (2005) 1139–1143.
[2] A.J. Engler, S. Sen, H.L. Sweeney, D.E. Discher, Matrix elasticity directs stem cell lineage specification, Cell. 126 (2006) 677–689.
[3] R.J. Pelham, Y. Wang, Cell locomotion and focal adhesions are regulated by substrate flexibility, Proc. Natl. Acad. Sci. 94 (1997) 13661–13665.
[4] S.L. Marshall, K.D. Schulze, S.M. Hart, J.M. Urueña, E.O. McGhee, A.I. Bennett, et al., Spherically capped membrane probes for low contact pressure tribology, Biotribology. 11 (2017) 69–72.
[5] A.C. Dunn, J.M. Uruena, Y. Huo, S.S. Perry, T.E. Angelini, W.G. Sawyer, Lubricity of surface hydrogel layers, Tribol. Lett. 49 (2013) 371–378.
[6] K. Schulze, S. Zehnder, J. Urueña, T. Bhattacharjee, W. Sawyer, T. Angelini, Elastic modulus and hydraulic permeability of MDCK monolayers, J. Biomech. 53 (2017) 210–213.
[7] T.G. Kuznetsova, M.N. Starodubtseva, N.I. Yegorenkov, S.A. Chizhik, R.I. Zhdanov, Atomic force microscopy probing of cell elasticity, Micron. 38 (2007) 824–833.
[8] D. Lucca, K. Herrmann, M. Klopfstein, Nanoindentation: measuring methods and applications, CIRP Ann. 59 (2010) 803–819.
[9] P.C. Nalam, N.N. Gosvami, M.A. Caporizzo, R.J. Composto, R.W. Carpick, Nano-rheology of hydrogels using direct drive force modulation atomic force microscopy, Soft Matter 11 (2015) 8165–8178.
[10] M. Garcia, K.D. Schulze, C.S. O'Bryan, T. Bhattacharjee, W.G. Sawyer, T.E. Angelini, Eliminating the surface location from soft matter contact mechanics measurements, Tribology-Materials, Surfaces & Interfaces. 11 (2017) 187–192.
[11] K.D. Schulze, A.I. Bennett, S. Marshall, K.G. Rowe, A.C. Dunn, Real area of contact in a soft transparent interface by particle exclusion microscopy, J. Tribol. 138 (2016) 041404.
[12] J. Boussinesq, Application des potentiels à l'étude de l'équilibre et du mouvement des solides élastiques, Gauthier-Villars, Imprimeur-Libraire, 1885.
[13] H.R. Hertz, Uber die Beruhrung fester elastischer Korper und Uber die Harte, Verhandlung des Vereins zur Beforderung des GewerbefleiBes, Berlin, 1882, p. 449.
[14] J. Harding, I. Sneddon, The elastic stresses produced by the indentation of the plane surface of a semi-infinite elastic solid by a rigid punch, Mathematical Proceedings of the Cambridge Philosophical Society, Cambridge University Press, 1945, pp. 16–26.
[15] I.N. Sneddon, The relation between load and penetration in the axisymmetric Boussinesq problem for a punch of arbitrary profile, Int. J. Eng. Sci. 3 (1965) 47–57.
[16] W.C. Oliver, G.M. Pharr, An improved technique for determining hardness and elastic modulus using load and displacement sensing indentation experiments, J. Mater. Res. 7 (1992) 1564–1583.
[17] W.C. Oliver, G.M. Pharr, Measurement of hardness and elastic modulus by instrumented indentation: advances in understanding and refinements to methodology, J. Mater. Res. 19 (2004) 3–20.
[18] D. Tabor, A simple theory of static and dynamic hardness, Proceedings of the Royal Society of London Series A Mathematical and Physical Sciences. 192 (1948) 247–274.
[19] A.M. Díez-Pascual, M.A. Gómez-Fatou, F. Ania, A. Flores, Nanoindentation in polymer nanocomposites, Prog. Mater. Sci. 67 (2015) 1–94.
[20] A.V. Dobrynin, J.-M.Y. Carrillo, Universality in nonlinear elasticity of biological and polymeric networks and gels, Macromolecules. 44 (2010) 140–146.
[21] K. Costa, F. Yin, Analysis of indentation: implications for measuring mechanical properties with atomic force microscopy, J. Biomech. Eng. 121 (1999) 462–471.
[22] C. Storm, J.J. Pastore, F.C. MacKintosh, T.C. Lubensky, P.A. Janmey, Nonlinear elasticity in biological gels, Nature. 435 (2005) 191.
[23] P.G. de Gennes, Soft matter (Nobel lecture), Angew. Chem. Int. Ed. Engl. 31 (1992) 842–845.
[24] Z. Duan, Y. An, J. Zhang, H. Jiang, The effect of large deformation and material nonlinearity on gel indentation, Acta Mech. Sinica 28 (2012) 1058–1067.
[25] S.Z. Bonyadi, M. Atten, A.C. Dunn, Self-regenerating compliance and lubrication of polyacrylamide hydrogels, Soft Matter (2019), https://doi.org/10.1039/C9SM01607D Advance Article.
[26] D. Lin, E. Dimitriadis, F. Horkay, Elasticity of rubber-like materials measured by

AFM nanoindentation, Express Polym Lett 1 (2007) 576–584.
[27] C.A. Charitidis, Nanoscale deformation and nanomechanical properties of polydimethylsiloxane (PDMS), Ind. Eng. Chem. Res. 50 (2010) 565–570.
[28] G. Chandrashekar, F. Alisafaei, C.S. Han, Length scale dependent deformation in natural rubber, J. Appl. Polym. Sci. 132 (2015).
[29] C.T. McKee, J.A. Last, P. Russell, C.J. Murphy, Indentation versus tensile measurements of Young's modulus for soft biological tissues, Tissue Eng. B Rev. 17 (2011) 155–164.
[30] M. Stolz, R. Raiteri, A. Daniels, M.R. VanLandingham, W. Baschong, U. Aebi, Dynamic elastic modulus of porcine articular cartilage determined at two different levels of tissue organization by indentation-type atomic force microscopy, Biophys. J. 86 (2004) 3269–3283.
[31] K.L. Johnson, K.L. Johnson, Contact Mechanics, Cambridge university press, 1987.
[32] M.R. VanLandingham, Review of instrumented indentation, Journal of Research of the National Institute of Standards and Technology. 108 (2003) 249.
[33] K.D. Schulze, S.M. Hart, S.L. Marshall, C.S. O'Bryan, J.M. Urueña, A.A. Pitenis, et al., Polymer osmotic pressure in hydrogel contact mechanics, Biotribology. 11 (2017) 3–7.